Modeling Surface Solar Radiation: Model Formulation and Validation

R. T. PINKER AND J. A. EWING

Department of Meteorology, University of Maryland, College Park, MD 20742

(Manuscript received 4 May 1984, in final form 30 October 1984)

ABSTRACT

A model for computing global solar radiation at the surface was formulated for use with satellite observations. A compromise in the approach was necessary, whereby the model accuracy and the inherent limitations of satellite observations were made compatible. A three-layer model atmosphere was used. The part of the solar spectrum from 0.3 to 0.7 μm was split into four equally spaced spectral intervals; the region from 0.7 to 4 μm was divided into eight nonspectral intervals. Use was made of the Delta–Eddington approximation, and parameterization was applied to the optical properties of Rayleigh scattering, water vapor absorption, aerosol absorption and scattering, and cloud absorption and scattering. Ozone absorption was also accounted for. The primary driving input of the model is the cloud optical depth, which can be inferred either from satellite observations (Experiment A) or from surface cloud observations (Experiment B). In Experiment A, the model was run for the months of May–August 1982 to produce estimates of daily cumulative insolation for Toronto, Canada. The mean value of the daily estimate was 19.61 MJ m^{-2} while the mean measured value was 19.72 MJ m^{-2}. The correlation between the predicted and measured daily totals was 0.944, and the standard error of estimate was 2.47 MJ m^{-2}, which is 12.5% of the mean observed value. Experiment B was run for the months May–August of 1981 and 1982. The standard errors of estimate were 16 and 18% of the respective means.

1. Introduction

Incident solar flux at the earth's surface is an important component of the net radiation which is a fundamental measure of the energy available at the earth–atmosphere interface. Net radiation regulates evapotranspiration, sensible heat flux, soil heat flux and photosynthesis. It is also relevant to problems dealing with climate trends, solar energy applications and agriculture. Information about surface radiative fluxes is needed at different temporal and spacial scales and at different accuracies. According to Leith (1978), climate models would benefit from radiation budget observations at an accuracy of 5% for a 1000 km spatial scale and a monthly mean time scale. Climate diagnostic studies require a horizontal resolution of 250 km at a daily time scale with 5% accuracy. The demands of the agricultural community call for a horizontal resolution of 20–50 km at a daily time scale within 10% accuracy. Since solar fluxes are observed only at a number of selected locations, there is a need for supplementing the available information.

Several models based on routine meteorological observations and/or satellite observations have been developed to estimate incident solar radiation (Atwater and Ball, 1981; Tarpley, 1979; Gautier *et al.*, 1980; Moser and Raschke, 1984). In the present study we formulated a computationally efficient radiative transfer model which allows us to estimate surface solar insolation on an hourly and daily basis, using as inputs routine meteorological or satellite observations. When compared to models developed previously for use with satellite data, it marks an improvement in the representation of the physical processes in the atmosphere. Details about the formulation of the model and parameterization of ozone, Rayleigh scattering, water vapor, aerosols and clouds are presented in Section 2. Test results of the model sensitivity to input parameters are given in Section 3. Data used for model formulation and testing are described in Section 4. Calibration of the GOES/VISSR is discussed in Section 5. Results from Experiment A (input from satellite observations) are presented in Section 6 and from Experiment B (input from ground observations) in Section 7.

2. The solar model

a. Model formulation

A number of techniques to deal with radiative transfer in a multiple scattering nonconservative atmosphere are available. Each of these schemes has an associated degree of complexity and accuracy as discussed in detail by Lenoble (1977). For our application, the Delta–Eddington technique was chosen since it marks an improvement in accuracy over the two-stream and conventional Eddington methods,

and since aerosol effects may easily be incorporated. Joseph *et al.* (1976) have tested the validity of the Delta–Eddington approximation for the following ranges of variables,

albedo of single scattering: $0.1 < \omega < 0.99$
asymmetry factor: $0 < g < 0.95$
optical thickness: $0.01 < \tau < 100$
cosine of solar zenith angle: $0.1 < \mu < 1$
surface albedo: $0 < A < 0.8$.

In these ranges the Delta–Eddington approximation was found to have an accuracy of better than 2.5% of the incident flux relative to the doubling method. However, the method can sometimes produce nonphysical values of upward diffuse flux (Wiscombe, 1977). The behavior of the approximation has also been investigated by Welch and Zdunkowski (1982) who have associated errors in the approximation with the convergence of the backscattering coefficients to their asymptotic limits.

For our application a three-layer model atmosphere is assumed. The levels of the model could be variable; in our experiments, they have been set at 0, 2 and 5.5 km with an additional level at the top of the atmosphere (Fig. 1). The solar spectrum from 0.3 to 0.7 μm is split into four spectral intervals (0.3–0.4, 0.4–0.5, 0.5–0.6 and 0.6–0.7 μm). The region from 0.7 to 4 μm is divided into eight nonspectral intervals based on a discrete probability distribution of water vapor absorption coefficients (Lacis and Hansen, 1974). A set of ω, τ and g is determined for each interval and each layer at any given time following Leighton (1979):

$$\tau = \sum \tau_i; \quad \omega = \sum \frac{\omega_i \tau_i}{\tau}; \quad g = \sum \frac{\omega_i \tau_i g_i}{\omega \tau}, \qquad (1)$$

where the subscript i refers to various radiatively important constituents. In this model the ω, τ, and g are parameterized for Rayleigh scattering, water vapor absorption, aerosol absorption and scattering, and cloud absorption and scattering. Ozone absorption effects are taken into account by reducing the incident solar flux in relevant spectral intervals. Water vapor absorption is assumed to be variable but aerosol effects are held constant due to a lack of information on aerosol variability.

In what is to follow, the parameterization for each constituent will be described in more detail.

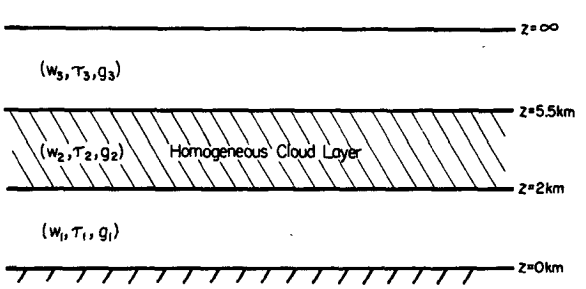

FIG. 1. Model atmosphere assumed for this study.

b. *Ozone parameterization*

Lacis and Hansen (1974) have presented analytical expressions for the percent of the solar flux absorbed as a function of ozone amount for the Chappuis band and for the ultraviolet absorption bands. Our model assumes a constant ozone amount of 0.4 cm. It is also assumed that the absorption associated with the Chappius band is contained within the 0.5–0.6 μm region. The total downward flux absorbed by this band A_c is then calculated using the following equation:

$$A_c = \frac{0.02118x}{1 + 0.042x + 0.000323x^2}, \qquad (2)$$

where x is the ozone amount transversed by the direct solar beam as is passes through the atmosphere, given as:

$$x = uM, \qquad (3)$$

u being the ozone amount in a vertical column from the surface to the top of the atmosphere and M a magnification factor defined as follows:

$$M = \frac{35}{(1223\mu^2 + 1)^{1/2}}, \qquad (4)$$

where μ equals the cosine of the zenith angle. The amount of energy which is absorbed is then subtracted from the incident flux in the 0.5–0.6 μm interval.

The fraction of the absorbed downward flux in the ultraviolet region due to ozone A_u is then calculated according to the following parameterization:

$$A_u = \frac{1.082x}{(1 + 138.6x)^{0.805}} + \frac{0.0658x}{1 + (103.6x)^3}. \qquad (5)$$

The flux in the wavelength region < 0.3 μm is assumed to be completely absorbed and the difference between this and the total amount absorbed by the ultraviolet ozone bands is subtracted from the incident flux in the 0.3–0.4 μm interval.

The percent of radiation absorbed by ozone according to this parameterization is generally below two. No account has been made in the model for additional absorption by ozone due to the reflected radiation coming from the lower atmosphere and the surface.

c. *Rayleigh scattering parameterization*

Effects due to Rayleigh scattering are considered for the four spectral intervals in the 0.3–0.7 μm

region. For Rayleigh scattering $\omega = 1$ and $g = 0$. The Rayleigh normal optical depth at any height and for any wavelength from that height to the top of the atmosphere is approximated following Margraff and Griggs (1969) as

$$\tau_r(\lambda, h) = 0.0088\lambda^{(-4.15+0.2\lambda)} \times \exp[-0.1188h - 0.00116h^2], \quad (6)$$

where λ is the wavelength (μm), h the altitude (km), and $\tau_r(\lambda, h)$ is the Rayleigh normal optical depth from altitude h to infinity.

The optical thickness for any of the spectral intervals is taken to be the average of the optical thickness appropriate for the endpoint wavelengths of those intervals. The effective Rayleigh optical thickness for each of the three atmospheric levels is then computed for the four spectral intervals by making use of (6).

d. Water vapor parameterization

It was assumed that there is no water vapor absorption for wavelengths < 0.7 μm. The energy associated with wavelengths > 0.7 μm was partitioned into eight intervals according to a discrete probability distribution of water vapor absorption coefficients (Lacis and Hansen, 1974). The total absorption due to water vapor in a layer containing y cm of precipitable water, $A(y)$, may then be approximated as

$$A(y) \approx 1 - \sum_{n=1}^{8} P(k_n)e^{-k_n y'}, \quad (7)$$

where k_n is a discrete absorption coefficient $P(k_n)$ represents the probability distribution for those discrete absorption coefficients, and y' is the effective water vapor path length.

The weight associated with the fraction of the incident flux where there is negligible water vapor absorption was adjusted to exclude the fraction of energy with wavelengths < 0.7 μm since that region was treated seperately. The water vapor optical thickness τ_n for any layer and for any interval n is given by

$$\tau_n = y'k_n, \quad (8)$$

where y' is the effective water vapor path length in that layer which was obtained from the precipitable water amount y of that layer by

$$y' = y\left(\frac{P}{P_0}\right)\left(\frac{T_0}{T}\right)^{0.5}. \quad (9)$$

Assumed vertical distributions of temperature T and pressure P were used to determine a mean pressure and temperature for each layer in order to allow the above scaling.

e. Aerosol parameterization

The aerosol parameterization follows the approach of Leighton (1979), who assumed a haze-C distribution of aerosols and used Mie theory calculations to obtain values for the aerosol asymmetry factor, albedo of single scattering and extinction coefficient $\beta(0)$ at the surface. These values are available for each of the four spectral intervals used. For the eight nonspectral intervals (wavelengths > 0.7 μm) they are assumed constant, since the form of the dependence of aerosol optical parameters on wavelength suggests that for the near-infrared (NIR) region a single set of parameters may adequately describe the aerosol effects. The model then assumes an idealized vertical distribution of aerosols, specifically, that the number of particles decreases exponentially with height. The aerosol optical thickness for any layer, $\tau(z_1, z_2)$, is calculated from the equation

$$\tau(z_1, z_2) = \int_{z_1}^{z_2} \beta(z)dz, \quad (10)$$

with the extinction coefficient $\beta(z)$ being approximated by

$$\beta(z) = \beta(0)e^{-z/H}, \quad (11)$$

where H is the effective aerosol scale height (the height through which the aerosol concentration drops off by a factor of e). An appropriate average scale height for the site was determined as detailed in Section 3c1.

f. Cloud parameterization

The treatment of cloud properties is very critical since, for a given zenith angle, clouds are the major determinants of the flux reaching the ground. The asymmetry factor for all clouds is assumed to be 0.85 for all wavelengths (Hansen and Pollack, 1970). Clouds are assumed to be nonabsorbent for wavelengths < 0.7 μm. Due to the manner in which the solar spectrum was divided, for wavelengths > 0.7 μm an albedo of single scattering had to be assigned independent of wavelength for the NIR interval. Stephens (1978) determined cloud albedos of single scattering for eight different cloud types and then averaged these values. The values were empirically derived as functions of cloud optical depth and solar zenith angle. The ω were appropriate for wavelengths > 0.75 μm and consequently were used in the present model for the NIR region. The ω were presented for the range of $1 < \tau < 500$ and $0.1 < \mu < 1$ and vary from 0.96 to 1 with a most frequently occurring value

near 0.98. The appropriate value would vary from cloud to cloud due to different drop size distributions and concentrations. The value most frequently used in the model for the NIR (0.98) does allow for amounts of cloud absorption compatable with current estimates of 10–20% (Liou, 1976). The sensitivity of the choice of the NIR ω for clouds is tested in Section 3d2.

Cloud optical thickness is to be inferred either from satellite observations (Experiment A), or from surface observations (Experiment B), as will be discussed in Sections 6 and 7.

3. Model sensitivity studies

It is important to determine the sensitivity of the model results to various model input parameters since the sensitivity will indicate to what precision these quantities must be known in order to closely simulate the actual surface fluxes.

a. Sensitivity to the zenith angle

The dependence of the global and diffuse surface flux and the upward flux at the top of the atmosphere on the solar zenith angle is shown in Fig. 2 for clear skies. The diffuse flux is seen to have a much weaker dependence on the zenith angle than does the global flux for most of the day. For very large zenith angles the diffuse flux accounts for the major part of the global flux.

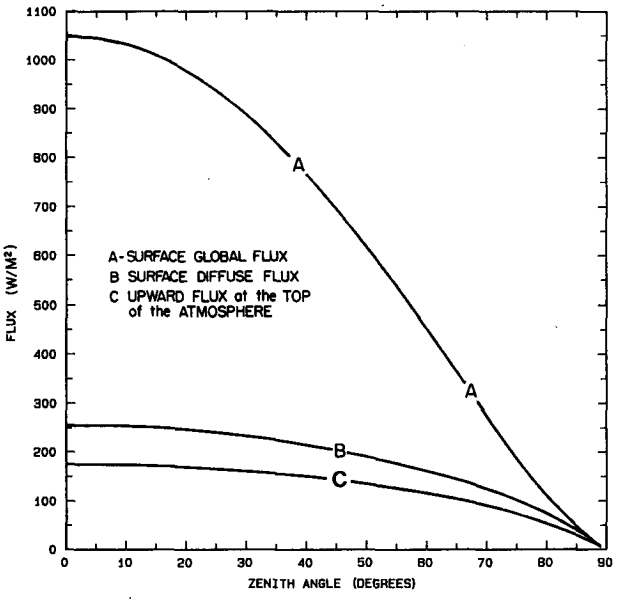

FIG. 2. Model-generated (A) surface global flux, (B) surface diffuse flux and (C) upward flux at the top of the atmosphere as a function of solar zenith angle. Surface albedo = 0.22; cloud optical thickness = 0; precipitable water = 1.40 cm; and Julian date = 140.

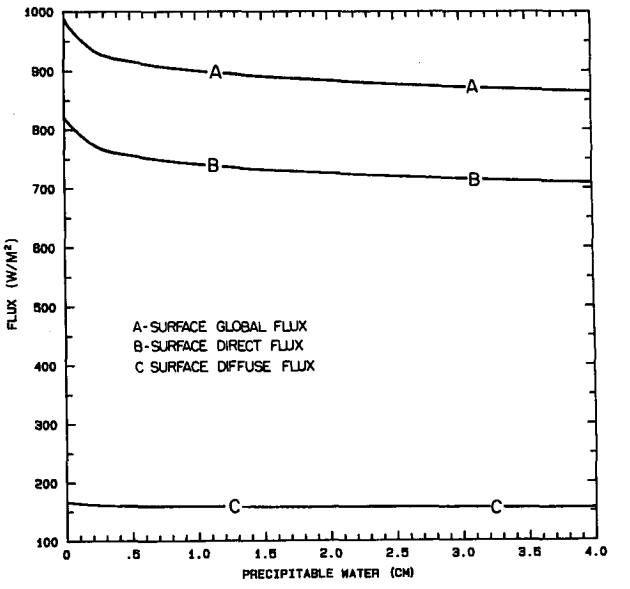

FIG. 3. Model-generated (A) surface global flux, (B) surface direct flux and (C) surface diffuse flux as a function of precipitable water. Surface albedo = 0.22; cloud optical thickness = 0; solar zenith angle = 30°; and Julian date = 140.

The upward flux at the top of the atmosphere has a zenith angle relationship similar to that for the surface diffuse flux. For large zenith angles the planetary albedo is higher than for small zenith angles, which causes the upward flux to depart from the cosine zenith angle relationship it would have were the planetary albedo constant. Since the time of the satellite observation is known only within an interval of 15 min, there is some error in the estimated zenith angle for each satellite measurement.

b. Sensitivity to precipitable water amount

The water vapor absorption estimated by the parameterization used in this model is of the order of 10% of the incident solar flux. The sensitivity of the surface fluxes to the precipitable water amount is illustrated in Fig. 3. Within the range of realistic water vapor amounts (0.75–4 cm) the three curves are nearly horizontal, indicating that the flux is not very sensitive to errors in the amount of precipitable water. Thus, a single daily value of precipitable water should be sufficient for our objective.

c. Sensitivity to the aerosol parameterization

1) SENSITIVITY TO THE AEROSOL SCALE HEIGHT

The sensitivity of the model results to the choice of aerosol scale height are illustrated in Fig. 4. As the

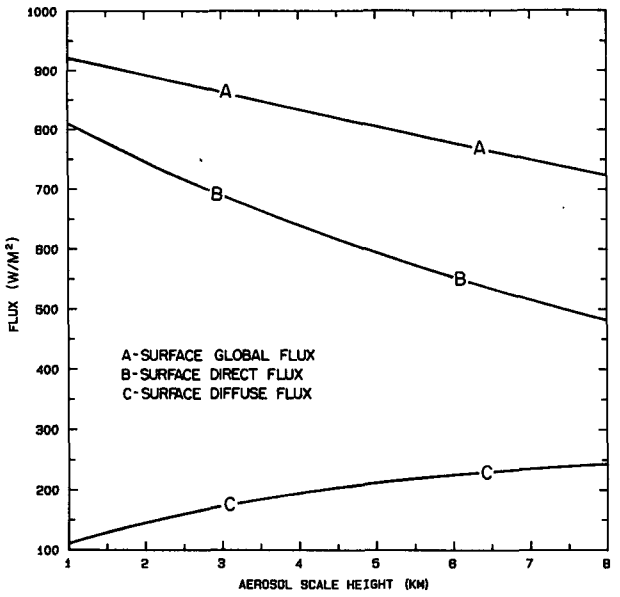

FIG. 4. As in Fig. 3 but as a function of aerosol scale height; precipitable water = 1.60 cm and Julian date = 200.

aerosol scale height increases, so does the total atmospheric aerosol loading since the surface properties are assumed to be constant. Direct flux decreases with increasing aerosol scale height due to increased absorption and scattering, while the diffuse flux increases. The global radiation is seen to decrease with increasing aerosol scale height since the decrease in the direct flux apparently outweighs the increase in the diffuse flux.

2) SENSITIVITY TO THE AEROSOL ASYMMETRY FACTOR AND ALBEDO OF SINGLE SCATTERING

The appropriate values for the aerosol ω and g are dependent on the type and distribution of aerosols.

TABLE 1. Sensitivity study of radiation fluxes to aerosol parameters of albedo of single scattering ω and asymmetry factor g. Surface albedo = 0.22; cloud optical thickness = 0; solar zenith angle = 30°; precipitable water = 1.40 cm; and Julian date = 140.

	Surface global flux (W m^{-2})	Surface diffuse flux (W m^{-2})	Upward flux at the top of the atmosphere (W m^{-2})
Original values	882	157	229
Values after all aerosol ω were decreased by 10%	857	140	215
Values after all aerosol g were decreased by 10% (with the ω restored)	876	164	234

In order to determine the sensitivity to the choice of these parameters first, all aerosol ω were decreased by 10% throughout the solar spectrum. The changes in the radiative fluxes for a given situation are illustrated in Table 1. Both the direct and diffuse components decreased due to additional absorption, causing the global flux to decrease by almost 3% (25 W m^{-2}). This change also decreased the planetary albedo by 6% of its original value. Reduction by 10% of all aerosol asymmetry factors led to more diffuse radiation at the ground (due to additional backscatter of reflected radiation from the surface) and a decrease of the direct flux (possibly due to greater photon path lengths). These two effects were partially canceling, resulting in a slight decrease in incident global flux. The planetary albedo had increased by a small amount due to additional backscatter (Table 1). Errors in the choice of asymmetry factor are apparently less critical than errors in the choice of the albedo of single scattering.

d. Sensitivity to cloud parameters

1) SENSITIVITY TO CLOUD OPTICAL THICKNESS

The sensitivity of the radiative flux to cloud optical thickness is illustrated in Fig. 5. The global and the diffuse flux at the ground and the upward flux at the top of the atmosphere are presented as functions of cloud optical thickness. It can be seen that as the

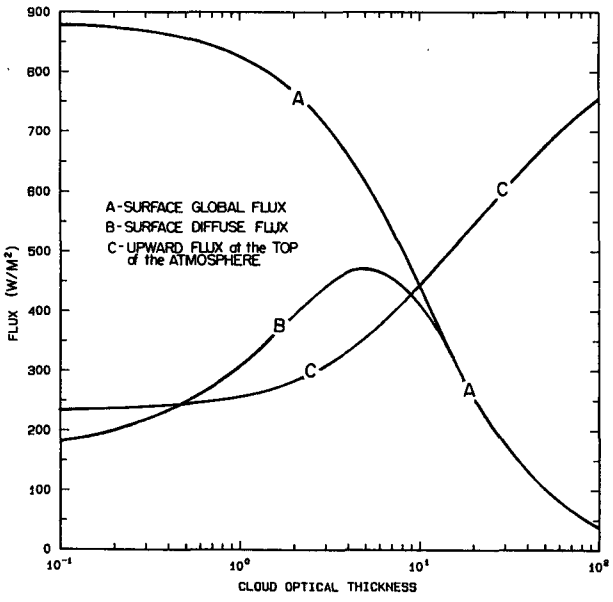

FIG. 5. As in Fig. 2 but as a function of cloud optical thickness. Surface albedo = 0.22; solar zenith angle = 30°; precipitable water = 1.40 cm; and Julian date = 140.

cloud optical thickness increases from 1 to 10, the incident flux at the surface is approximately halved, while the upward flux at the top of the atmosphere is almost doubled. As the cloud optical thickness increases to 100 and beyond, the global surface flux approaches zero and the total atmospheric absorption approximates 20%. For large optical thickness the global flux consists almost entirely of diffuse radiation since the direct flux is strongly attenuated. The diffuse flux itself is seen to increase for a while with increasing optical thickness due to additional scattering; then to decrease due to attenuation of the scattered radiation. For a given cloud optical thickness of 10, a 10% increase of this value (for a zenith angle of 30°) would decrease the model computed surface flux from 426 W m^{-2} to 399 W m^{-2}, a 6% error. The estimation of a proper cloud optical thickness for any situation is the most crucial aspect of this model.

2) Sensitivity of the global flux to cloud NIR albedo of single scattering

As stated in Section 2f, the cloud albedo of single scattering is assumed to be 1 for wavelengths < 0.7 μm, and for the NIR (wavelengths > 0.7 μm) it is expressed as a function of cloud optical thickness and zenith angle following Stephens (1978). There would also be variations in the NIR cloud ω due to unresolved variations in cloud particle characteristics. The sensitivity of the global surface flux to ω is shown in Fig. 6. For a small optical thickness, changes in ω within the range presented (0.96–0.999) are not very important (the path length is small, resulting in small cloud absorption). For optical thickness > 1 the choice of ω becomes critical, indicating the importance of reliable cloud ω estimates.

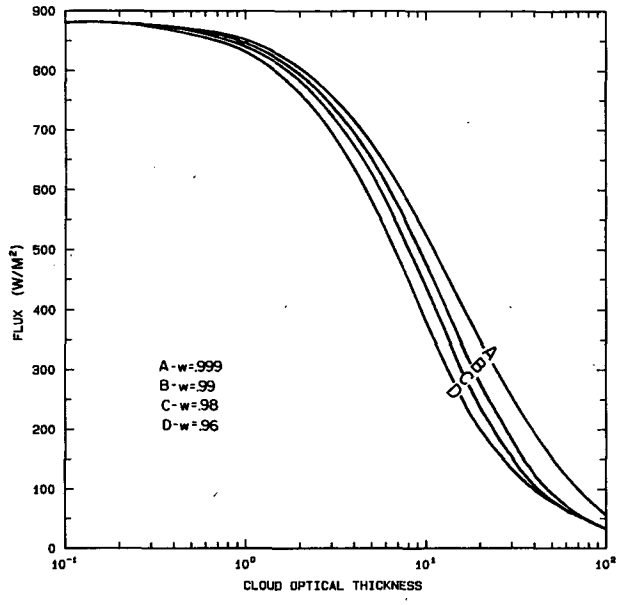

FIG. 6. Model-generated surface global flux as a function of cloud optical thickness with cloud NIR albedo of single scattering equal to (A) 0.999, (B) 0.990, (C) 0.980, (D) 0.960. Surface albedo = 0.22; solar zenith angle = 30°; precipitable water = 140 cm; and Julian date = 140.

e. *Sensitivity to the surface albedo*

The model was run with different surface albedos, holding all other inputs constant. A linear relationship between the planetary albedo a_p and the surface albedo a_s was obtained for several selected zenith angles in the range from 0–80°. A linear relationship is also reported by Braslau and Dave (1973), Preuss and Geleyn (1980), and Chen and Ohring (1984). The effects of surface albedo on the global flux at the surface S_g were also tested. Once again, linear relationships were obtained. The accuracy requirements for the surface albedo would depend on whether one is concerned with surface or planetary flux. For a surface albedo of 0.20, an uncertainty of 10% changes the planetary albedo by 7%, while the surface global flux changes by 3/10% only.

4. Data

Surface and satellite data were collected during a two year period (1981–82) at the following sites in Canada: Elora, 43°39′N, 80°25′W; Ottawa, 45°27′N, 75°31′W; Sable Island, 43°56′N, 60°00′W; St. Augustin, 46°44′N, 71°30′W; and Toronto, 43°48′N, 79°33′W. In the present study only data from Toronto and Ottawa were utilized.

The surface data were obtained from the Canadian Climate Center of the Atmospheric Environment Service (Phillips and Aston, 1980). The surface radiation data for Toronto consist of hourly cumulative values of global solar radiation, diffuse solar radiation, and reflected solar radiation. For Ottawa, diffuse and reflected radiation measurements were not available. Surface albedo was computed as the ratio of reflected radiation to global radiation, and was found to average 22% for the Toronto site (which is located on a farm 10 miles east of the city). The diffuse radiation was used to estimate an appropriate average aerosol scale height for the site since no information was available about the vertical distribution of aerosols. It is assumed that the aerosols have a haze-C size distribution with known properties at the surface and an exponential decrease with height of the extinction coefficient. For a number of clear days in Toronto, the model was run with varying aerosol scale height (holding all other parameters constant) until the predicted and measured values of global and diffuse radiation at the surface were in good agreement. The estimated values range from 1.4 to 2.6 km; the value of 2.4 km was chosen as representative.

The hourly surface cloud observations consist of low cloud layer type and amount, second cloud layer type and amount, and total cloud amount. There were 17 possible cloud types. For daytime hours at Toronto for the period of May–August 1981 we find the following situation: 8% of the hours are clear, 18% of the hours the predominate cloud type is altostratus, 14% cirrus, 22% cumulus, 19% stratocumulus, and 19% other cloud types. The mean cloud amount for daytime hours during this period is 6.9 tenths.

The satellite data set contained 8 km resolution Visible and Infrared Spin Scan Radiometer (VISSR) pixels from the GOES-E. The VISSR is a scanning radiometer that is stepped from north to south and uses the rotation of the satellite to scan from west to east. It makes measurements in two wavelength regions: an interval in the visible region (0.55–0.75 μm), and one in the thermal IR window region (10.5–12.5 μm). The satellite data were collected as part of an experimental program and are not routinely available. The selected resolution and format were based on experience obtained during a previous experiment over the Great Plains (Tarpley, 1979).

Eleven visible observations are collected each day for each site. The data are in the form of counts which are dimensionless quantities proportional to the square root of the filtered intensity in the associated spectral region. The visible count values are on a scale from 0 to 63 and were found to lie within a range of 14 to 57 for the daytime hours studied in the 1982 period for Toronto. Both the mean count values of 5×5 arrays of pixels and the count values for the center pixel of the array were collected. These two values are generally very similar, differing by no more than 10%. Each array of pixels covers an area on the surface of about 50 km on a side and centered at the latitude and longitude of the surface sites. The 8 km resolution data were used in this study. The GOES data collected have an accurate predetermined navigation (i.e., a proper location is assigned to each radiation measurement). Along with every count value is provided the appropriate time of the observation, an associated solar zenith, angle a satellite azimuth angle, and daily estimates of the atmospheric precipitable water amount as obtained from the National Meteorological Center (NMC) analysis.

5. Calibration of the GOES instruments

Numerous calibrations have been performed for the GOES/VISSR over the years since sensor response varies from satellite to satellite and the response of any single sensor changes with time. Two calibration procedures were experimented with in this study, and will be described in the following sections.

- Calibration 1. Abel (1983) presented a prelaunch calibration for the satellite data used in this study (i.e., GOES-5). The first step in this procedure is a conversion from counts into volts. Since the satellite reports nonzero count values when viewing deep space (6.5 counts) it is necessary to subtract 0.06 volts. Subsequently, the voltages are transformed to narrowband albedos using a calibration determined by the Santa Barbara Research Corporation.
- Calibration 2. Smith *et al.* (1981) presented a calibration of the visible counts from the GOES-1 satellite in terms of spectrally integrated shortwave fluxes. The calibration is based upon space and time coincident radiation measurements from an aircraft. The aircraft carried narrowband and broadband narrow-angle directional radiometers and broadband flux radiometers (Ackerman and Cox, 1980). The application of the calibration calls for the transformation of the visible counts into narrowband (0.55–0.75 μm) reflectance; association of a broadband reflectance (0.3–4 μm) with the narrowband reflectance, according to the type of the underlying surface; and transformation of the directional broadband reflectance to an angularly integrated albedo (assuming isotropy). We used the transformation that was appropriate for vegetation.

In order to assess the differences between the two calibrations, a comparison was made whereby the planetary albedo was computed for a given VISSR count, using each calibration independently. The results indicate (Fig. 7) that the derived albedos are in close agreement, in particular over the count range of 35 to 45. This was unexpected since the Abel procedure does not apply a narrow to broadband conversion or an angular integration.

6. Experiment A: model input from GOES observations

a. Procedures

In Experiment A the GOES-E VISSR data were used to estimate cloud optical thickness. A relationship between planetary albedo, cloud optical thickness and zenith angle was derived, and used to estimate appropriate cloud optical thickness for a known planetary albedo and zenith angle. The solar model discussed in Section 2 was run to produce planetary albedos for various values of cloud optical thickness and zenith angle. The determined functional relationship is shown in Fig. 8 for a surface albedo of 25%. This value of surface albedo was adopted since when used in our model, it yielded a planetary albedo which was in good agreement with the planetary albedo derived from the clear-sky satellite observations via the calibration equation. A value of 22% was obtained as the average measured surface albedo for the Toronto experimental site. However, we require a value

that would be appropriate for the 8 km pixels sensed by the satellite; this might differ from the point measurement value. A value of 25% for the summer surface albedo for Toronto is also reported by Hay (1983).

Once the planetary albedo is determined, cloud optical thickness may be inferred, and used with the known vapor amount, zenith angle and other assumed parameters to predict the surface fluxes. A similar procedure was employed by Curran and Wu (1982) who determined cloud reflection as a function of a scaled optical thickness and a similarity parameter. They calculated the reflection function by using the doubling method of Hansen (1971) for a particular geometric situation. If the reflection function is known, the scaled optical thickness of clouds may be inferred according to the numerically derived relationship.

For Experiment A, our model was run to compute global flux for each hour of the day from 0630 to 1730 LST. Cloud optical thickness for any given hour was inferred from the satellite observation which was closest to that hour. It was assumed that the flux calculated at the middle of an hourly interval was equal to the hourly averaged flux from which hourly insolation was estimated. All hourly insolation values for a given day were then summed to obtain the daily cumulative insolation.

b. Results of Experiment A

1) GLOBAL SOLAR RADIATION-HOURLY PREDICTION

Experiment A was performed with the Abel calibration to produce pairs of hourly values of measured and predicted global fluxes for May–June 1982 for Toronto. This data set consisted of 456 cases. The mean measured flux was 417 W m^{-2}; the mean predicted flux was 414 W m^{-2}; the correlation coefficient for the measured and predicted hourly values was 0.814; and, the standard error of estimate is 155 W m^{-2}, which is 37% of the mean measured value.

When Experiment A was performed with the Smith *et al.* calibration, the mean predicted flux was 411 W m^{-2}; the correlation coefficient was 0.827; and the standard error of estimate was 150 W m^{-2}, which is 36% of the mean measured value.

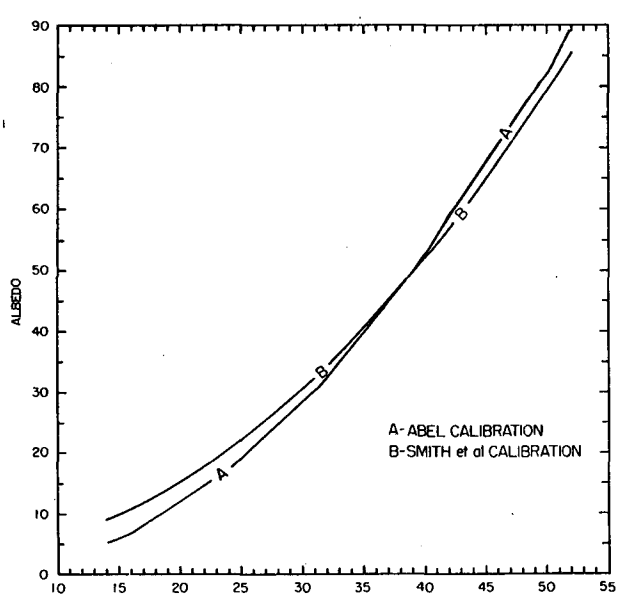

FIG. 7. Planetary albedo as a function of the VISSR visible count using (A) Abel calibration (B) Smith *et al.* calibration.

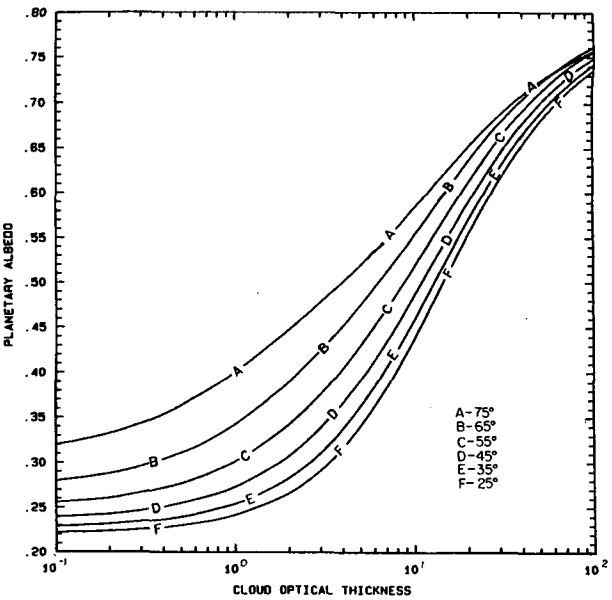

FIG. 8. Model-generated planetary albedo as a function of cloud optical thickness for various solar zenith angles. Surface albedo = 0.25; precipitable water amount = 1.40 cm; and Julian date = 140.

2) GLOBAL SOLAR RADIATION—DAILY PREDICTION

Experiment A was performed with each calibration to produce estimates of daily cumulative insolation for May–August 1982 for the Toronto site (92 days). When run with the Abel calibration, the mean value of the daily estimate was 19.61 MJ m^{-2}, compared to a mean measured value of 19.72 MJ m^{-2}. The correlation between the predicted and measured daily values was 0.944. The standard error of estimate is 2.47 MJ m^{-2}, which is 12.5% of the mean observed value. With the Smith *et al.* calibration, the mean estimate was 19.45 MJ m^{-2}, the correlation coefficient was 0.948, and the standard error of estimate was 2.39 MJ m^{-2}, which is 12.1% of the mean observed value.

The performance of the model on a daily basis is illustrated for Toronto, August 1982 in Fig. 9, and for the whole four-month period in Fig. 10.

Experiments were conducted where the standard error of estimate was computed using different averaging periods ranging between one and ten days. The results are presented in Fig. 11. As evident, when the averaging period increased, the standard error of estimate decreases, ranging between 16–5% for time intervals ranging from one to ten days. One should however note that for an averaging period of ten days, the sample was rather small (only six cases). The least square fit line was obtained by giving appropriate weight to each data point according to the number of cases it represents.

7. Experiment B: model input from ground observations

a. Procedures

In Experiment B use is made of surface observations of cloud type and cloud amount as the primary forcing functions of the predicted surface insolation. Approximate range of optical thickness for several cloud types was determined from aircraft measurements by Feigelson (1977). Nimbostratus has an associated value of 70, stratus and stratocumulus have a range of 9–21, and altostratus and altocumulus have a range of 9–31. The exact value would depend on the microphysics of the clouds. Since we had no information on the variations in cloud particle characteristics, a single value of optical thickness had to be assigned for each cloud type. We had the option of either taking the arithmetic mean of the endpoints of the specified range, or computing the global fluxes

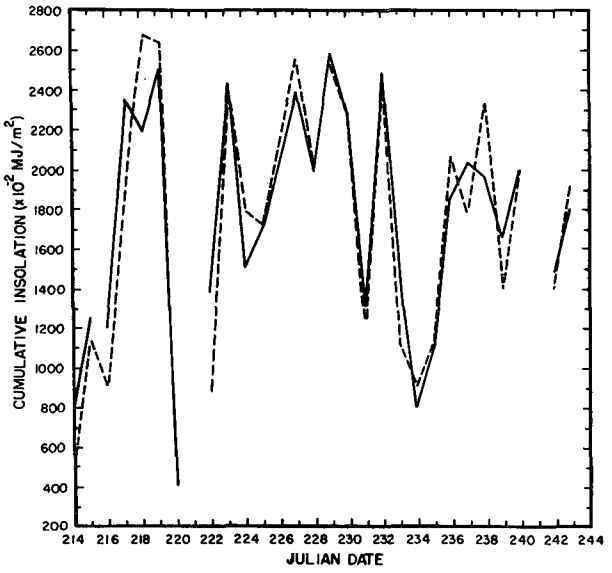

FIG. 9. Measured (solid) and Experiment A-estimated (dashed) values of daily cumulative insolation for Toronto for the month of August 1982 using Abel's calibration.

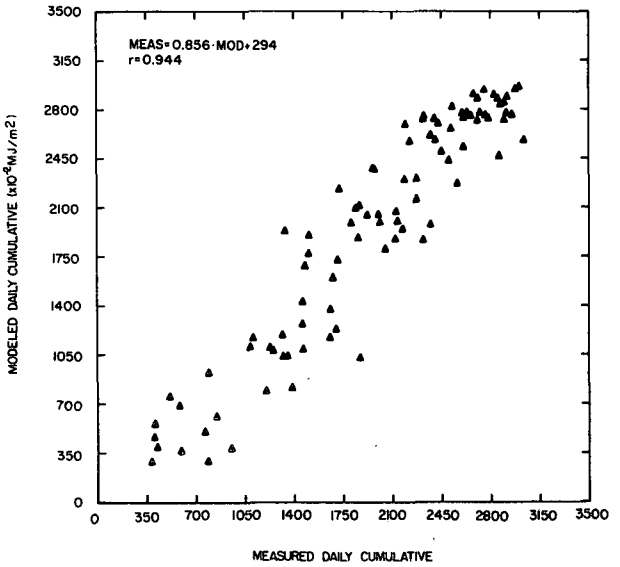

FIG. 10. Scattergram of measured and Experiment A-estimated values of daily cumulative insolation for Toronto for the period of May through August 1982 using Abel's calibration.

for the endpoints, averaging these fluxes, and then using an optical thickness associated with this average flux. It was found that the second method gave better results when compared with actual measurements, and it was therefore adopted for this experiment. For cumulonimbus a value of 30 as suggested by Peng *et al.* (1982) was adopted. In order to estimate optical thickness for cloud types for which information is not available, cases were isolated in our data base for which a particular cloud type was predominant. Our model was run with varying cloud optical thickness until the differences between the measured and observed values approached zero. Generally, only overcast conditions of a given cloud type were analyzed (except for cumulus clouds). Joseph and Davies (1980) reported for cumulus clouds experimentally derived optical thickness ranging from 4 to 150. For a seven day period in June in which cumulus clouds were predominant we found that an optical thickness of 3 was most appropriate. For these partly cloudy situations, reflection from the sides of clouds may tend to increase the surface global flux, and thus a one-dimensional model would require a smaller cloud optical thickness than measured in order to reproduce the observed fluxes. The values we used in our experiment for each cloud type are shown in Table 2.

At any particular time, the global flux was computed for overcast skies of the predominant cloud type and for clear skies. These two flux values were weighted according to cloud amount and added to produce the model estimated flux.

The model was run to compute global flux for every hour of each day from 0630 to 1730 LST. As

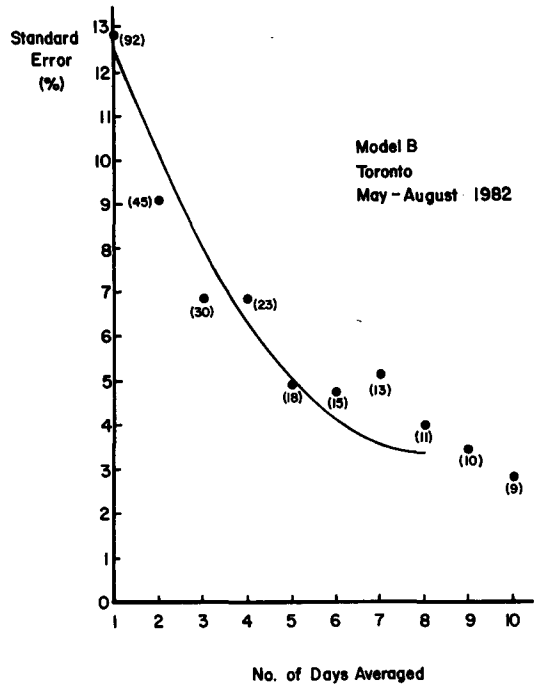

FIG. 11. Standard errors SE of estimate for the global solar radiation obtained in Experiment A for Toronto, as a function of the number of days d averaged (SE = 0.19 d^2 − 2.95 d + 15.10). The solid line represents a second-order least-square fit. Each point was weighted according to the number of cases it represents (in parentheses).

in Experiment A, it was assumed that the instantaneous flux computed at the center of an hourly interval was equal to the hourly averaged flux from which the hourly insolation was estimated. All hourly insolation values for a given day were then summed to obtain the daily cumulative insolation. The surface radiation observations were used to estimate the ratio of the cumulative total from sunrise to sunset to the twelve hourly cumulative total. From May through August, this ratio ranged from 1.000 to 1.099, with a mean value of 1.022. This mean value was used to correct the estimated 12 hourly sums into estimated daily totals.

b. Results of Experiment B

1) GLOBAL SOLAR RADIATION—HOURLY PREDICTION

Hourly predicted and measured fluxes for the first half of May for Toronto (120 cases) were analyzed to reveal a correlation coefficient of 0.826. The mean measured hourly flux was 430 W m^{-2}; the mean predicted flux was 385 W m^{-2}; and the standard error of estimate was 148 W m^{-2} (34% of the mean observed).

2) GLOBAL SOLAR RADIATION—DAILY PREDICTION

Experiment B was performed to produce estimates of daily cumulative insolation for Toronto for the months of May–August 1981 and 1982. In Fig. 12, the model estimated and ground observed values of daily cumulative insolation for Toronto for the month of June 1981 are illustrated.

The daily values for the four months of 1981 for Toronto (111 cases) were grouped together and analyzed statistically. The correlation between the predicted and observed daily totals is 0.919. The mean observed value is 19.37 MJ m^{-2} and the mean predicted value is 19.10 MJ m^{-2}. The standard error of estimate is 3.17 MJ m^{-2}, which is 16% of the mean observed value. A scattergram was also gener-

TABLE 2. Values of cloud optical thickness assigned to overcast skies of each of the listed cloud types. The assignments were based either on literature survey or experimental fits to available data.

Code	Symbol	Cloud type	Cloud optical thickness	Basis of assignment
1	AC	Altocumulus	20	Feigelson (1977)
2	ACC	Altocumulus Castellanus	23	1 day in July 1981
3	AS	Altostratus	20	Feigelson (1977)
4	CC	Cirocumulus	1	1 day in June 1981
5	CS	Cirrostratus	15	2 days in May 1981
6	CI	Cirrus	1	month of May 1981
7	CB	Cumulonimbus	30	Peng *et al.* (1982)
8	CU	Cumulus	3	7 days in June 1981
9	CF	Cumulus fractus	24	6 days in May 1981
10	SF	Stratus fractus	42	2 days in July 1981
11	TCU	Towering cumulus	10	2 days in June 1981
12	NS	Nimbostratus	70	Feigelson (1977)
13	SC	Stratocumulus	15	Feigelson (1977)
14	ST	Stratus	15	Feigelson (1977)
15	F	Fog	4	1 day in June 1981; 1 day in July 1981

ated (Fig. 13); the best-fit line to the data points had a slope of 0.994 and an intercept of 31 W m^{-2}.

In order to assess the performance of the model with an independent data set and different location, the experiment was performed for July 1981 for Ottawa (Fig. 14), assuming the same aerosol properties as were estimated for Toronto. Statistical analysis of the results (28 cases) shows that the correlation of predicted and observed daily totals is 0.938; the mean observed value is 20.34 MJ m^{-2}; and the mean predicted value is 19.39 MJ m^{-2}. The standard error of estimate is 2.57 MJ m^{-2}, which is 13% of the mean observed value. A comparison of these results with those for Toronto indicates that the overall results for both locations are in agreement.

The daily values for the four months of 1982 for Toronto (86 cases) were also grouped together and analyzed statistically. The correlation between the predicted and observed daily totals is 0.884. The mean observed value is 19.70 MJ m^{-2} and the mean predicted value is 19.59 MJ m^{-2}. The standard error of estimate is 3.55 MJ m^{-2}, which is 18% of the mean observed value.

In order to compare objectively the results of Experiment A and Experiment B, we selected those days for which the necessary model input parameters were available for both tests. Within the four month period of May–August 1982 at Toronto, there was a total of 86 days for which both measured values of daily cumulative insolation and estimated values from both experiments were available. The relevent statistics are presented in Table 3. It is evident that the results from Experiment A have a lower standard error than the corresponding results from Experiment B.

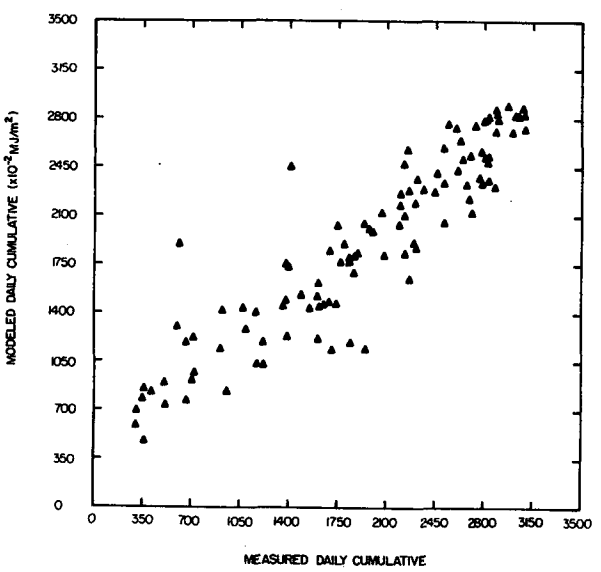

FIG. 13. Scattergram of Measured and Experiment B-estimated values of daily cumulative insolation for Toronto for the period of May through August 1981.

8. Summary

A radiative transfer model has been formulated to compute radiative fluxes for various states of a model

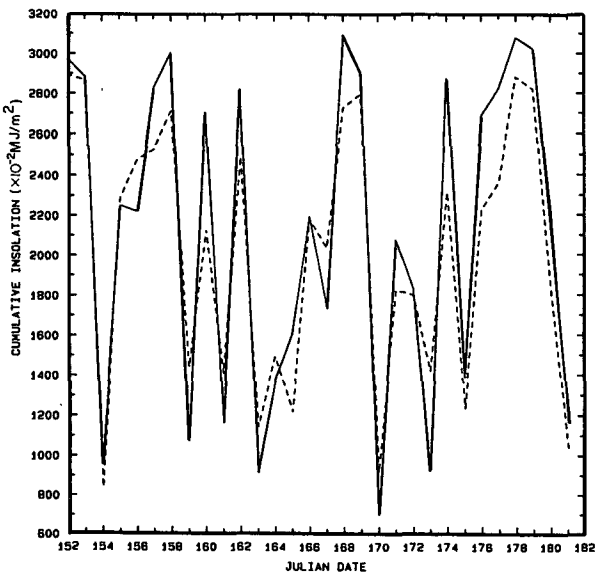

FIG. 12. Measured (solid) and Experiment B-estimated (dashed) values of daily cumulative insolation for Toronto for the month of June 1981.

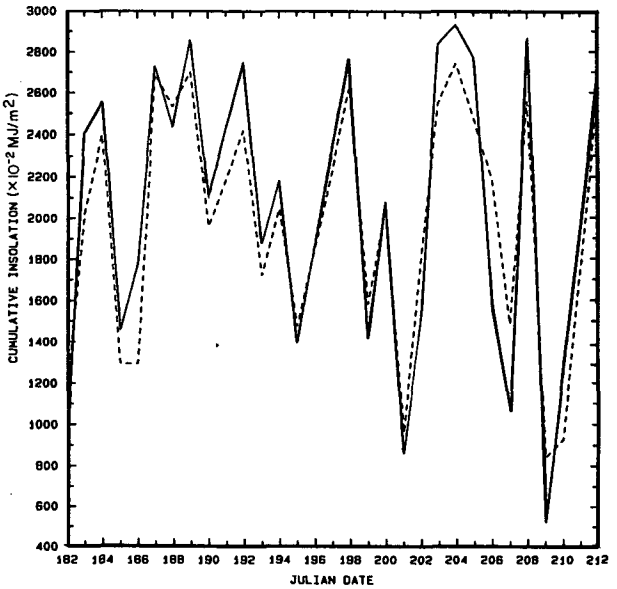

FIG. 14. Measured (solid) and Experiment B-estimated (dashed) values of daily cumulative insolation for Ottawa for the month of July 1981.

TABLE 3. Summary of regression analysis between the measured values of daily cumulative insolation and estimated values from Experiment A and Experiment B for 86 days during May–August 1982 at Toronto, Canada.

	Cases	Mean daily insolation (MJ m^{-2})	Correlation coefficient	Standard error
Measured	86	19.70		
Predicted				
Experiment A	86	19.25	0.95	12%
Experiment B	86	19.59	0.88	18%

atmosphere. This model incorporates parameterizations for ozone absorption, Rayleigh scattering, water vapor absorption, aerosol absorption and scattering and cloud absorption and scattering. Sensitivity studies conducted with this model have shown that zenith angle and cloud optical thickness are the most important input parameters to the model. Cloud NIR single scattering albedo is also important and should be estimated properly. Accurate aerosol parameterization is important under clear skies, otherwise cloud effects dominate the radiative transfer process. Water vapor absorption should be taken into account, but small errors in the precipitable water may be tolerated. The requirements for the accuracy of the surface albedo are shown to be dependent on the objective of the computations, having stronger effect on the planetary albedo than on the surface global flux.

Test results of the model were presented for two experiments. In Experiment A, the optical thickness was inferred from satellite observations; in Experiment B, the ground based cloud observations were used to drive the model.

In Experiment A use was made of the GOES-E VISSR data to estimate cloud optical thickness using a model-derived relationship between planetary albedo and optical thickness. Once the optical thickness is inferred from the observed planetary albedo, it can be used with all the other model parameters (measured or assumed) to predict the surface fluxes. Experiment A was performed to produce pairs of hourly values of measured and predicted global fluxes. The data set consisted of 456 hourly cases taken during the May and June 1982 period for Toronto. The mean measured flux was 417 W m^{-2}; the mean predicted flux was 411 W m^{-2}; the correlation coefficient for the measured and predicted hourly values was 0.827; and the standard error of estimate was 150 W m^{-2}, which is 36% of the mean measured value.

Experiment A was implemented to produce pairs of daily values of measured and predicted insolation. The data set consisted of 92 cases taken during May–August 1982 for Toronto. The mean measured daily insolation was 19.72 MJ m^{-2}; the mean predicted insolation was 19.61 MJ m^{-2}; the correlation coefficient for the measured and predicted daily values was 0.944; and the standard error of estimate was 2.47 MJ m^{-2}, which is 12.5% of the mean observed value.

In Experiment B use was made of surface observations of cloud type and cloud amount to estimate surface fluxes. Experiment B was performed to produce pairs of hourly values of measured and predicted global fluxes. The data set consisted of 120 cases taken during May 1982 for Toronto. The mean measured flux was 430 W m^{-2}; the mean predicted flux was 385 W m^{-2}; the correlation coefficient for the measured and predicted hourly values was 0.826; and the standard error of estimate was 48 W m^{-2} which is 34% of the mean observed value.

Experiment B was implemented to produce pairs of daily values of measured and predicted insolation. The data set consisted of 111 cases taken during May–August 1981 for Toronto and 86 cases taken during May–August 1982 for Toronto. For the first group (1981) the correlation between the predicted and observed daily totals was 0.919 and the standard error of estimate was 16% of the mean observed value. For the second group (1982) the correlation between the predicted and observed daily totals was 0.884 and the standard error of estimate was 18% of the mean observed value.

Acknowledgments. This work was supported by Grant NA80AA-D-0048 from NOAA/NESDIS under project AGRISTARS. We are thankful to the granting agency and to the Computer Science Center of the University of Maryland, College Park, for providing supplementary computer time.

REFERENCES

Abel, P. G., 1983: Prelaunch radiance calibration of VISSR/VAS. NOAA/NESS Tech. Note E/RA22, 7 pp.

Ackerman, S., and S. K. Cox, 1980: Colorado State University radiation instrumentation and data reduction procedures for the CV-990 during summer MONEX. Atmos. Sci. Pap. 325, Colorado State University, Fort Collins, CO, 72 pp.

Atwater, M. A., and J. T. Ball, 1981: A surface solar radiation model for cloudy atmospheres. *Mon. Wea. Rev.*, **109**, 878–888.

Braslau, N., and J. V. Dave, 1973: Effect of aerosols on the transfer of solar energy through realistic model atmospheres. Part I: Non-absorbing aerosols. *J. Appl. Meteor.*, **12**, 601–615.

Chen, T. S., and G. Ohring, 1984: On the relationship between clear-sky planetary and surface albedos. *J. Atmos. Sci.*, **41**, 156–158.

Curran, R. J., and M. L. Wu, 1982: Skylab near-infrared observations of clouds indicating supercooled liquid water droplets. *J. Atmos. Sci.*, **39**, 635–647.

Feigelson, E. M., 1977: Preliminary radiation model of a cloudy atmosphere. Part I: Structure of clouds and solar radiation. *Beitr. Phys. Atmos.*, **51**, 203–229.

Gautier, C., G. Diak and S. Masse, 1980: A simple physical model to estimate incident solar radiation at the surface from GOES satellite data. *J. Appl. Meteor.*, **19**, 1005–1012.

Hansen, J. E., 1971: Multiple scattering of polarized light in planetary atmospheres. Part 1: The doubling method. *J. Atmos. Sci.*, **28**, 120–125.

——, and J. B. Pollack, 1970: Near-infrared light scattering by terrestrial clouds. *J. Atmos. Sci.*, **27,** 265–281.

Hay, J., 1983: *Introduction to Solar Radiation.* M. Iqbal, Ed., Academic Press, 252 pp.

Joseph, J. H., and R. Davies, 1980: The albedo of broken cumulus cloud fields. *Int. Radiation Symp.*, Fort Collins, 3 pp.

——, W. J. Wiscombe and J. A. Weinman, 1976: The Delta–Eddington approximation for radiative flux transfer. *J. Atmos. Sci.*, **33,** 2452–2459.

Lacis, A. A., and J. E Hansen, 1974: A parameterization for the absorption of solar radiation in the Earth's atmosphere. *J. Atmos. Sci.*, **31,** 118–133.

Leighton, H. G., 1979: Application of the Delta–Eddington method to the absorption of solar radiation in the atmosphere. *Atmos.-Ocean,* **18,** 43–52.

Leith, C. E., 1978: Earth radiation budget science 1978. *Proc. NASA/Langley Workshop,* Williamsburg, NASA/Langley, 72 pp.

Lenoble, J., Ed., 1977: Standard procedures to compute atmospheric radiative transfer in a scattering atmosphere. Radiation Commission, IAMAP, National Center for Atmospheric Research, 125 pp.

Liou, K. N., 1976: On the absorption, reflection and transmission of solar radiation in cloudy atmosphere. *J. Atmos. Sci.*, **33,** 798–805.

Margraff, W. A., and M. Griggs, 1969: Aircraft measurements and calculations of the total downward flux of solar radiation as a function of altitude. *J. Atmos. Sci.*, **26,** 469–477.

Moser, W., and E. Raschke, 1984: Incident solar radiation over Europe estimated from METEOSAT data. *J. Climate Appl. Meteor.*, **23,** 166–170.

Peng, L., M. D. Chou and A. Arking, 1982: Climate studies with a multi-layer energy balance model. Part I: Model description and sensitivity to the solar constant. *J. Atmos. Sci.*, **39,** 2639–2656.

Phillips, D. W., and D. Aston, 1980: Canadian solar radiation data. Environment Canada, 1–15.

Preuss, H. J., and J. F. Geleyn, 1980: Surface albedos derived from satellite data and their impact on forecast models. *Arch. Meteor. Geophys. Bioklim.*, **A29,** 345–356.

Smith, W. L., L. D. Herman, T. Schreiner, H. B. Howell and P. Menzel, 1981: Radiation budget characteristics of the onset of the summer monsoon. *Int. Conf. on Early Results of FGGE and Large Scale Aspects of its Monsoon Experiments.* Tallahassee, 11 pp.

Stephens, G. L., 1978: Radiation profiles in extended water clouds. Part II: Parameterization schemes. *J. Atmos. Sci.*, **35,** 2123–2132.

——, 1979: Estimating incident solar radiation at the surface from geostationary satellite data. *J. Appl. Meteor.*, **18,** 1172–1181.

Welch, R. M., and W. G. Zdunkowski, 1982: Backscattering approximations and their influence on Eddington-type solar flux calculations. *Beitr. Phys. Atmos.*, **55,** 28–42.

Wiscombe, W. J., 1977: The Delta-Eddington approximation for a vertically inhomogeneous atmosphere. NCAR Tech. Note 121, 1–66.